Chemical Science

Accepted Manuscript

ROYAL SOCIETY OF CHEMISTRY

rsc.li/chemical-science

View Article Online
DOI: 10.1039/C8SC00745D

Journal Name

ARTICLE

"Waiting" Carbon Nitride Radical Anion: Charge Storage Material and Key Intermediate in Direct C-H Thiolation of Methylarenes Using Elemental Sulfur as "S"-source

Received 00th January 20xx,
Accepted 00th January 20xx

DOI: 10.1039/x0xx00000x

www.rsc.org/

Aleksandr Savateev,*[a] Bogdan Kurpil,[a] Artem Mishchenko,[b] Guigang Zhang[a] and Markus Antonietti[a]

Potassium poly(heptazine imide), a carbon nitride based semiconductor with high structural order and valence band potential of +2.2 V vs. NHE, in the presence of hole scavengers and under visible light irradiation gives corresponding polymeric radical anion, in which specific density of unpaired electrons reaches up to 112 μmol·g^{-1}. The obtained polymeric radical anion is stable under anaerobic conditions for several hours. It was characterized by UV-vis absorption, time resolved and steady state photoluminescence spectra. The electronic structure of the polymeric radical anion was confirmed by DFT cluster modelling. The unique property of potassium poly(heptazine imide) to store charges was employed in visible light photocatalysis. A series of substituted dibenzyldisulfanes was synthesized in 41-67% yields from corresponding methylarenes *via* cleavage of methyl C—H bond under visible light irradiation and metall free conditions.

Introduction

C—H functionalization of hydrocarbons mediated by heterogeneous visible light photocatalyst is highly tempting for sustainable chemistry.[1] This strategy can afford high value-added chemicals from inexpensive reagents, minimize the number of steps and hence auxiliary chemicals, reduce the number of by products and potentially could use only sun light as energy source, while the photocatalyst can be easily separated from the solution and used again.[2] Numerous examples of heterogeneous photocatalysts and photocatalytic reactions were reported in literature – hydrogen evolution reaction[3, 4] and overall water splitting,[5] CO_2 reduction[6, 7] and styrene production, just to name a few.[8] Due to chemical inertness, arising from very high C—H bond energies and ionization potentials, selective functionalization of hydrocarbons is quite challenging.[9]

Literature, describing C—H functionalization of hydrocarbons mediated by heterogeneous photocatalysts, is mostly represented by synthesis of aldehydes, ketones and carboxylic acids, since O_2 in all these cases is used as an electron scavenger and hydrogen oxidation as the thermodynamic driving force.[10-13]

In order to transcend the borders of heterogeneous photocatalysis applied to organic synthesis and to broaden the spectrum of products, semiconductors with high oxidation power of photogenerated holes may be envisioned for use. According to this strategy, potent thermodynamic driving force for substrate oxidation is created, eliminating the need in O_2, while mild electron acceptors can be then used to remove the electron from the conduction band (CB) and close the photocatalytic cycle.

In this view, potassium poly(heptazine imide), K-PHI hereafter (Fig. 1a),[14] a carbon nitride based material, is a promising candidate to assay this strategy.[15-17] The band structure of K-PHI is schematically shown in Fig. 1d. Due to highly positive valence band (VB) potential, +2.22 V vs. NHE, photogenerated holes are effective oxidants to apply in organic synthesis. For example, K-PHI was successfully used to oxidize alcohols to aldehydes and 1,4-dihydropyridines to pyridines,[18] in synthesis of 1,3,4-oxadizoles by oxidative cyclization of *N*-acylhydrazones,[19] in thioamides synthesis by photocatalytic Kindler reaction,[20] as well as in oxygen and hydrogen evolution reactions.[21]

On the other hand, CB in K-PHI is located at -0.5 V vs. NHE that is significantly lower compared, for example, to g-CN, -1.29 V vs. NHE. Therefore, it is reasonable to assume that K-PHI radical anion, hereafter denoted as K-PHI$^{\bullet-}$, formed from K-PHI upon its single electron reduction, would be stable and have lifetime above μs-s time scale (Fig. 2).[22] The viability of this idea was recently proved by Lotsch et. al who have reported radical carbon nitride specie with a lifetime exceeding hours, while the material was applied in hydrogen

[a] Department of Colloid Chemistry, Max-Planck Institute of Colloids and Interfaces Am Mühlenberg 1 14476 Potsdam, Germany, E-mail: oleksandr.savatieiev@mpikg.mpg.de
[b] Department for Heterophase Synthesis of Inorganic Compounds and Materials V.I. Vernadsky Institute of General and Inorganic Chemistry, Palladina Ave., 32/34, Kiev, 03680, Ukraine

Electronic Supplementary Information (ESI) available: XPS, UPS and FT-IR spectra of K-PHI, N_2 absorption isotherm, DFT calculations, toluene oxidative thiolation optimization results, material characterization after photocatalytic tests, ^{1}H and ^{13}C NMR spectra of disulfanes. See DOI: 10.1039/x0xx00000x

View Article Online
DOI: 10.1039/C8SC00745D

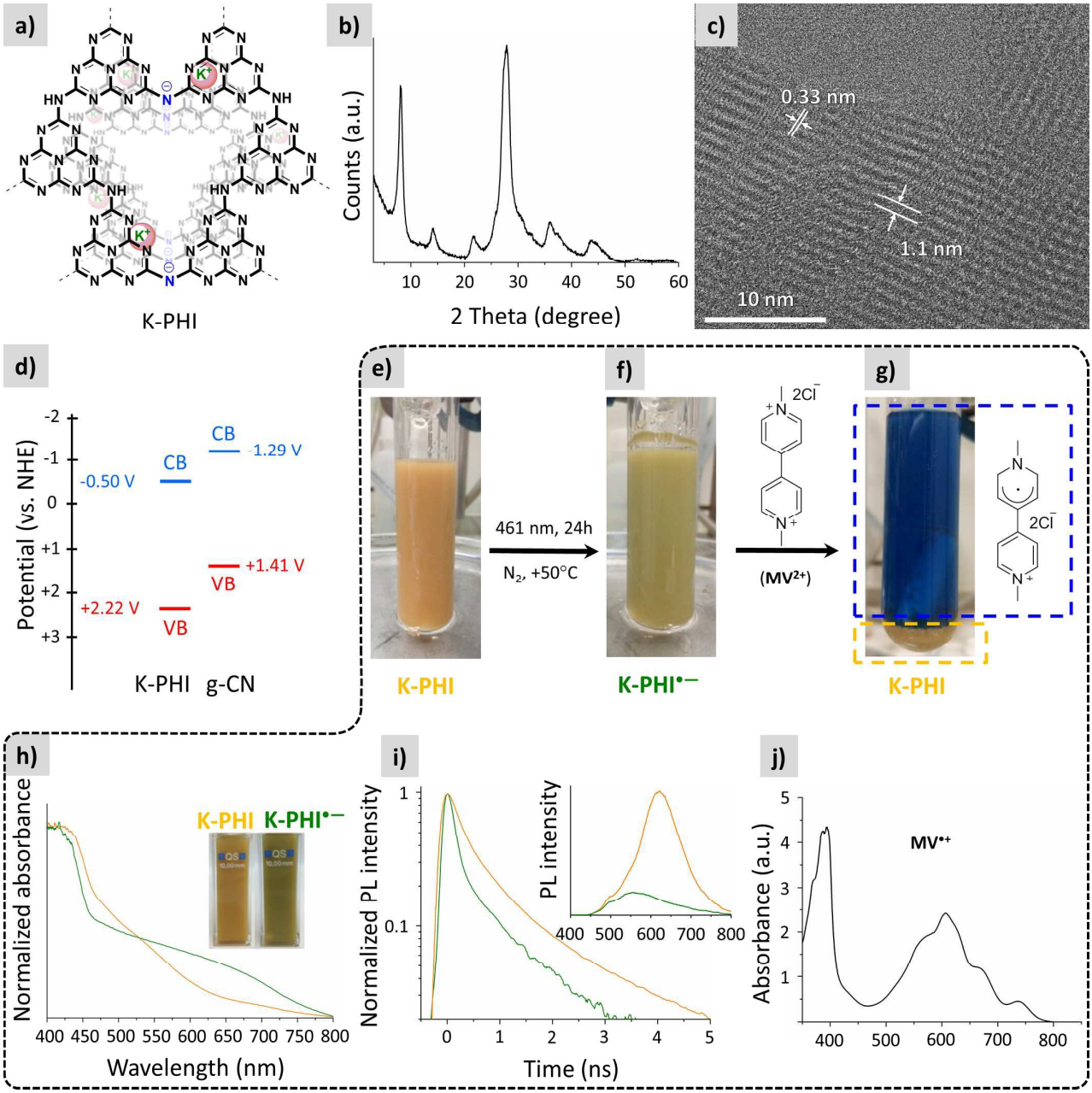

Fig. 1. a) Idealized structure of K-PHI. b) PXRD pattern of K-PHI. c) HR-TEM image of K-PHI. d) Band structure of K-PHI. CB position of K-PHI determined by Mott-Schottky analysis[15] and VB position calculated as $E_{VB} = E_{CB}$ + BG, where BG is the optical band gap of K-PHI determined from Tauc plot (Figure S1e). CB and VB potentials of g-CN were taken from the literature.[14] e) Suspension of K-PHI (10.39 mg), 4-methylanisole (0.6 mL) in acetonitrile (6.05 mL). f) The same suspension after stirring at +50°C, for 24 h under light irradiation (461 nm, $0.0517 \pm 3 \cdot 10^{-5}$ W·cm^{-2}). g) The same suspension immediately after methylviologen dichloride dihydrate (6.9 mg, 24 µmol) addition. Blue rectangle shows solution of $MV^{\bullet+}$ in acetonitrile, orange rectangle – precipitated K-PHI. h) UV-vis absorption spectra of K-PHI suspension in 4-methylanisole/MeCN mixture: prior irradiation (orange, suspension appearance is also shown in Fig. 1e) and after irradiation for 2h with 461 nm LED (green, suspension appearance is also shown in Fig. 1f), both recorded under anaerobic conditions. i) Time resolved PL spectra of K-PHI suspension in 4-methylanisole/MeCN mixture: prior irradiation (orange, suspension appearance is also shown in Fig. 1e) and after irradiation for 2h with 461 nm LED (green, suspension appearance is also shown in Fig. 1f), both recorded under anaerobic conditions. Steady state PL spectra of suspended materials, recorded using 360 nm excitation wavelength, given as inset. Experiments aimed to check ability of K-PHI to store electrons without external energy input under anaerobic conditions are enclosed with dashed line

evolution reaction and sun light harvesting device.[23, 24]

In the view of hydrocarbons C—H bond activation, the long living K-PHI$^{\bullet-}$ might be a key intermediate to use reagents, different from abovementioned O_2. The mechanism describing this approach is summarized in Fig. 2.

In the present work, we have shown that K-PHI in the presence of hole scavengers, even such weak as toluene, when triggered by visible light, acts as a capacious electron buffer and forms stable under air-free conditions radical anion. This feature was applied in visible light photocatalytic activation of C—H bond

View Article Online
DOI: 10.1039/C8SC00745D

of hydrocarbons – we have developed a simple and convenient method to synthesize dibenzyldisulfanes from inexpensive methylarenes and S_8 under visible light irradiation using K-PHI as a heterogeneous photocatalyst under metal free conditions.

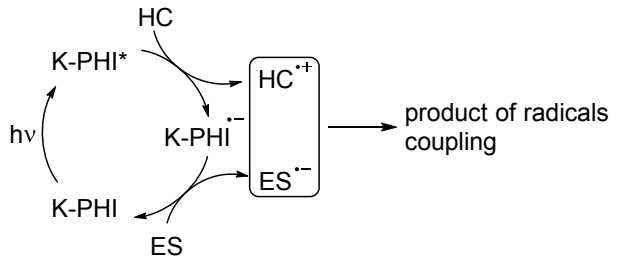

Fig. 2. A schematic representation of the photocatalytic reaction proceeding via reductive quenching of the photocatalyst. K-PHI* represents excited state of the photocatalyst, K-PHI$^{\bullet-}$ - radical anion, HC stands for "hydrocarbon", ES – electron scavenger.

Results and discussion

K-PHI was prepared according to the procedure reported by us earlier.[18] Powder X-Ray (PXRD) pattern demonstrates typical for this material diffraction peaks.[25] Among them intense peak at ~27° is due to stacking of layers similar to graphitic carbon nitride (g-CN), and peaks at 8.1°, 14.2°, 21.8°, 36.0° and 43.9° are related to ordered in-layer arrangement (Fig. 1b).[25] High resolution TEM image reveals crystalline structure of the synthesized K-PHI with interlayer distances of 0.33 nm and in plane periodicity of 1.1 nm (Fig. 1c). X-Ray photoelectron, ultraviolet photoelectron, diffuse reflectance UV-vis absorption, photoluminescence, Fourier-transform infrared (FT-IR) spectra, N_2 absorption isotherm and SEM image of K-PHI are given in the supporting information (Fig. S1) and they are consistent with the reported previosusly.[14, 26, 27]

In order to check the possibility to use K-PHI as electron buffer and subsequently to be engaged in photocatalytic hydrocarbons functionalization, we have performed the following experiment. A mixture of K-PHI, *p*-methylanisole (holes scavenger) in acetonitrile was mixed, degassed and kept under N_2 atmosphere during the whole experiment (Fig. 1e).[‡] The suspension was irradiated with 461 nm LED. After irradiation was stopped, we noticed that suspended particles of K-PHI have changed colour from orange to "avocado green" (Fig. 1f). Colour change was taken as a first evidence of the K-PHI radical anion formation, hereafter denoted as K-PHI$^{\bullet-}$.[23] Upon addition of the excess of dimethylviologene dichloride dehydrate (MV^{2+}), yellow K-PHI immediately precipitated, while solution changed its colour to intense blue, which is due to MV^{2+} single electron reduction to its radical cation ($MV^{\bullet+}$) (Fig. 1g). Measuring the absorbance of the solution at λ = 606 nm (Fig. 1j) and taking into account the extinction coefficient of $MV^{\bullet+}$ in acetonitrile of ε=13900,[28] the specific number of electrons stored by the polymeric K-PHI$^{\bullet-}$ was calculated to be 112 µmol per gramm of the material. In the control experiment, when MV^{2+} and K-PHI were mixed together prior irradiation, no $MV^{\bullet+}$ formed. However, MV^{2+} was converted into $MV^{\bullet+}$ upon subsequent light irradiation. It implies that energy input is essential to enable electron flux. Note, that the capacity of the covalent g-CN in the same experiment was orders of magnitude lower.

The optical properties of the suspended K-PHI$^{\bullet-}$ (Fig. 1f) were investigated. Thus, UV-vis absorption spectrum (Fig. 1h) shows a broad absorption band in the range 600-750 nm, which is in agreement with the observed green colour. Photoluminescence (PL) life-time of K-PHI$^{\bullet-}$ is 0.35 ns versus 0.66 ns for K-PHI (Fig. 1i). Room temperature steady-state PL spectrum of the K-PHI$^{\bullet-}$ suspension is significantly lower compared to K-PHI in the ground state, while the maximum is shifted to shorter wavelength (555 nm). This observation supports that *p*-methylanisole indeed acts as hole scavenger – it depopulates the number of holes and hence reduces PL.

We have observed colour change of the suspension from green back to yellow when suspension was exposed to S_8 or O_2 implying that these molecules can be used in combination with K-PHI in subsequent functionalization of hydrocarbons (shown below).

In order to characterize theoretically electronic structure of K-PHI, we have conducted a density functional theory (DFT) study on a model K-PHI cluster containing 6 heptazine units and 2 potassium ions. Its geometry was optimized using several pure (PBE, BLYP) and hybrid (PBE0, B3LYP, BHHLYP) generalized gradient approximation (GGA) functionals (see Experimental section and ESI file for details).

To a first approximation the energies of the highest occupied (HOMO) and lowest unoccupied (LUMO) molecular orbitals of the model cluster can be compared with the edge energies of K-PHI valence and conduction bands respectively. These

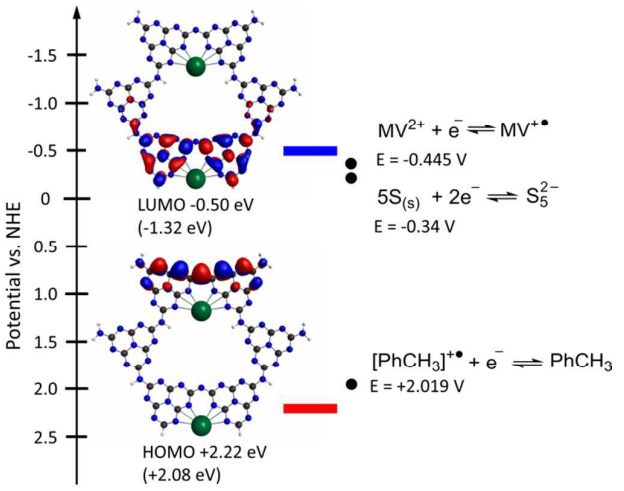

Fig. 3. CB position determined by Mott-Schottky analysis[15] and VB position calculated as $E_{VB} = E_{CB}$ + BG, where BG is the optical band gap, 2.72 eV, of K-PHI determined from Tauc plot (Figure S1e). HOMO and LUMO positions in K-PHI cluster predicted by PBE0 functional are given for comparison in parentheses. HOMO and LUMO positions from the Table 1 were recalculated taking into account an absolute value for the normal hydrogen electrode V_{NHE} = 4.18 V. Standard oxidation potential of toluene, MV^{2+} and sulfur were adapted from the literature.[29-31]

View Article Online
DOI: 10.1039/C8SC00745D

Journal Name

ARTICLE

Table 1. Computed orbital energies for the K-PHI cluster (eV in the absolute vacuum scale)

Value	PBE	PBE0	BLYP	B3LYP	BHHLYP
E_{HOMO}	–5.33	–6.26	–5.17	–5.99	–7.13
E_{LUMO}	–3.62	–2.86	–3.48	–2.97	–1.90
$\Delta E_{HOMO-LUMO}$	1.71	3.40	1.69	3.02	5.22

orbitals are of the π-type and located mainly on the nitrogen atoms of the poly(heptazine imide) matrix (Fig. 3). Among the used functionals, B3LYP gave the best agreement with the optical band gap determined experimentally, 3.02 eV vs. 2.72 eV (Table 1). On the other hand, PBE0 revealed that the HOMO of K-PHI cluster is located at 2.08 eV, which is comparable with the valence band position, +2.22 eV, obtained by adding optical band gap value, 2.72 eV (Figure S1e), to the conduction band value, -0.5 eV. Moreover, this valence band position agrees well with the VBM, +2.40 eV, determined directly using ultraviolet photoelectron spectroscopy (UPS) (Figure S1d). Since HOMO position is slightly more positive than oxidation potential of toluene (or even more positive than that of *p*-methylanisole, due to M+ effect of the OMe group), electron transfer from toluene to the valence band of K-PHI is thermodynamically allowed (Fig. 3). On the other hand, the predicted LUMO position is -1.32 eV and is significantly more negative than CB potential, -0.5 eV, measured using Mott-Schottky analysis.[15] Nevertheless, the reduction potential of MV^{2+} to $MV^{\bullet+}$, -0.445 V, is less negative than the CB potential, therefore reduction of sulfur by the photogenerated electrons from the CB of K-PHI is thermodynamically allowed.

The model reaction of K-PHI$^{\bullet-}$ quenching by adding MV^{2+}, O_2 or S_8, allows to call K-PHI a "waiting" photocatalyst, in terms that in the presence of hole scavenger, even such a weak one as *p*-methylaniosle, and light energy input, it is rapidly converted into stable K-PHI$^{\bullet-}$ and "waits" until oxidant comes to recover ground state of K-PHI.

Having the evidence that K-PHI is a capacious electron buffer and hence can decouple oxidation and reduction of the substrates, we applied this material in photocatalytic thiolation of toluene. Instead of using sulfur-transferring reagents, we took aim at elemental sulfur (S_8) as a cheap raw source. Its redox chemistry is well known and the problem of its utilization exist – the annual excess of sulfur production is about seven millions ton.[32] Instead of simply store it, chemists are seeking for the possibilities to utilize this huge excess of sulfur as an alternative feedstock for polymeric materials,[33] as electron sacrificial agent in photocatalysis[18] and so forth.[34]

Toluene, having oxidation potential of +2.019±0.02 V (vs. NHE) and relatively reactive methyl group,[29] has been chosen as a model substrate to screen the reaction conditions. The main results of these tests are summarized in Tables S1, S2. The formation of dibenzyldisulfide was unambiguously proved by the identity of its ^{13}C NMR, FT-IR and mass spectra to the reference (Fig. S2).

The developed photocatalytic system is indeed versatile and tolerant to different functional groups. A series of substituted methylarenes was converted into the corresponding disulfanes (Fig. 4). Dibenzyldisulfane **1a** was obtained in 56% isolated yield, while *p*-methoxysubstituted disulfane **1b** was obtained with even higher, 67%, yield. Interestingly, that steric effect is negligible and 1,2-bis(2-methoxybenzyl)disulfane **1c** was isolated with 63% yield. Ethylbenzene was exclusively oxidized at the α-position of the alkyl chain furnishing disulfane **1d**. This result again supports the idea that upon oxidation of alkylarene by K-PHI, first reactive specie of benzyl-type is formed, which subsequently reacts with sulfur. Disulfane **1d** was isolated as 1:1 mixture of its diastereomers as proven by ^{13}C NMR because K-PHI does not possess chirality. *p*-fluorotoluene was oxidized to disulfane **1e** with 41% isolated yield. *tert*-butyl *p*-tolylcarbamate gave the corresponding disulfane **1f** with 51% isolated yield implying that K-PHI offers quite mild conditions, under which the protection group remains intact. In case of *p*-toluonitrile the yield of disulfane **1g** was 9%, because the reaction terminated at the stage of polysulfane formation (see below). Finally, *p*-iodotoluene gave disulfane **1h**, though with ca. 3% yield, apparently due to

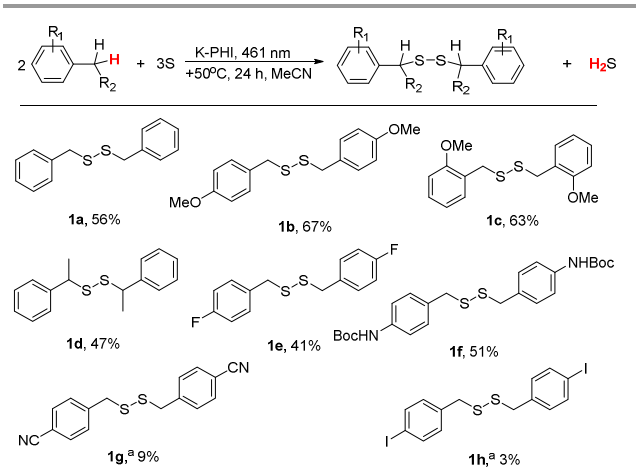

Fig. 4. Diaryldisulfane synthesis. Isolated yields are given unless other specified. Conditions: K-PHI 10 mg, methylarene 0.3 mL, S_8 0.96 mg, MeCN 2.7 mL, +50°C, 24 h, 461 nm ($0.0517\pm3\cdot10^{-5}$ mW·cm^{-2}). [a] determined by ^1H NMR using dibenzylether as an internal standard.

View Article Online
DOI: 10.1039/C8SC00745D

lability of C—I bond under photoredox conditions.

The highest yield of 1,2-dibenzyldisulfane was obtained when toluene oxidation was conducted under blue (461 nm) light (Fig. 5a), as this wavelength matches the K-PHI optical band gap, 2.72 eV. UV light (350 nm) gave disulfane with slightly lower yield, which could be rationalized by consecutive S—S bond cleavage under the highly energetic UV radiation. On the other hand, under green light (522 nm) almost no disulfane was generated. The apparent quantum yield (AQY) of *p*-methylanisole photooxidation at 461 nm was calculated to be 0.23±0.02% (Fig. 5a). Our calculations are based on photon flux measured using optical power meter equipped with integrating sphere and taking into account that every polysulfane molecule requires oxidation of two *p*-methylanisole molecules. It indicates that C—H bond oxidation at nearly room temperature is a difficult process especially in the absence of any metal co-catalysts, but still possible due to K-PHI.

All this behavior indicates that, contrary to photochemical water splitting with g-CN, this time the reduction process is the slow, rate determining step, as there is obviously no straight chemical reaction channel for the sulfur to quickly take up the photogenerated electron to restore the ground state of the photoredox catalyst.

Hammett plot (Fig. 5b) supports that the reaction is sensitive to electronic effects. The ρ constant is -0.75, suggesting that the rate limiting step involves positively charged species – the radical cation of benzyl type.

In the reaction mixture we have detected intermediate polysulfanes, namely 1,4-bis(4-methoxybenzyl)tetrasulfane and 1,3-bis(4-methoxybenzyl)trisulfane, when oxidation of *p*-methylanisole was studied. Given that chemical shift of the methylene groups depends on the number of sulfur atoms between the benzylic fragments, a peak at 4.13 ppm was assigned to 1,4-bis(4-methoxybenzyl)tetrasulfane CH_2 group,[35] while the one at 4.01 ppm – to the CH_2 group of 1,3-bis(4-methoxybenzyl)trisulfane[36] (Fig. 5c). The designed photocatalytic system can also produce polysulfides with up to 5 sulfur atoms when excess of sulfur was used (Fig. S3).

The time dependent composition of the reaction mixture is shown in Fig. 5d. Already after 86 min, 50 % of sulfur was consumed. However, the yield of disulfane was only 30 % of the theoretical, suggesting that at the beginning of the reaction sulfur is rapidly converted into polysulfides and stored in the form of bis(4-methoxybenzyl)polysulfanes. Nevertheless, the intermediate tetra- and trisulfides were completely converted into 1,2-bis(4-methoxybenzyl)disulfane after ca. 27 h of irradiation, implying that disulfane is the most stable under given photocatalytic conditions. The amount of target disulfane is asymptotically reaching the theoretical value, expected for the given amount of sulfur, and after 44 h 93 % of the maximum possible quantity were obtained, proving that the stoichiometric ratios between reagents and products are indeed as described in Fig. 4.

Summarizing all above mentioned observations, the tentative mechanism of methylarenes photocatalytic oxidative thiolation is shown in Fig. 6. Visible light excites K-PHI giving rise to K-PHI* species with a bound electron-hole exciton pair. At this point two pathways, oxidative and reductive quenching of K-PHI*, are in principle possible.[37] However, the reaction proceeds predominantly via the oxidation of methylarene (ArMe) to the corresponding radical cation ($ArMe^{\bullet+}$) which occurs relatively fast. The leftover $K\text{-}PHI^{\bullet-}$ is oxidized by S_8 back to the initial K-PHI, closing the photocatalytic cycle, while sulfur is then converted into $S_8^{\bullet-}$ (structure **a** on Fig. 6). We are aware that in solution sulfur can form polysulfides of different length as well as cyclic molecules,[38, 39] but for the clarity of presentation we assume that linear $S_8^{\bullet-}$ is the only product of sulfur reduction. Due to the positive charge, $ArMe^{\bullet+}$ is much stronger acid (pKa = -13, $PhCH_3^{\bullet+}$ in MeCN)[40] compared to the neutral ArMe (pKa = 54, $PhCH_3$, in MeCN).[41]

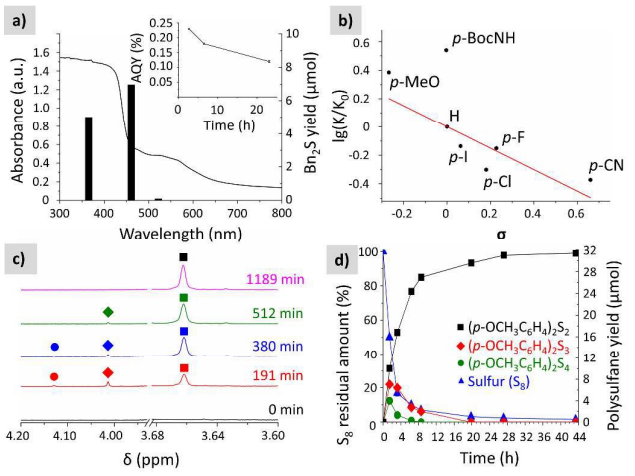

Fig. 5. (a) Diffuse reflectance UV-vis spectrum of K-PHI with yield of 1,2-dibenzyldisulfane depending on the irradiation wavelength. (b) Hammett plot. (c) Time dependent evolution of methylene group signal of $(p\text{-}OCH_3C_6H_4)_2S_2$ (squares), $(p\text{-}OCH_3C_6H_4)_2S_3$ (diamonds) and $(p\text{-}OCH_3C_6H_4)_2S_4$ (circles) in selected ^{1}H NMR spectra of the reaction mixture. (d) Time dependent yield of $(p\text{-}OCH_3C_6H_4)_2S_2$ (squares), $(p\text{-}OCH_3C_6H_4)_2S_3$ (diamonds) and $(p\text{-}OCH_3C_6H_4)_2S_4$ (circles), and residual sulfur (triangles).

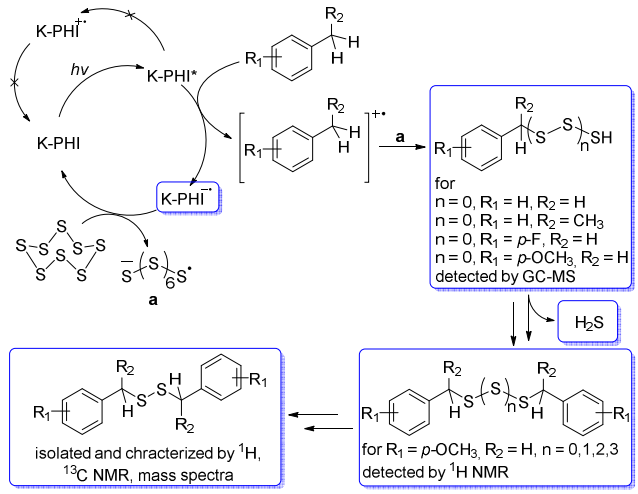

Fig. 6. A proposed mechanism of photocatalytic thiolation of toluene with elemental sulfur. Organic molecules or intermediate reactive species that were detected or isolated during the reaction course are highlighted with rectangles.

View Article Online
DOI: 10.1039/C8SC00745D

On the other hand, $S_8^{\bullet-}$, similar to the well-studied trisulfur radical anion $S_3^{\bullet-}$,[42] is basic and therefore abstracts proton from $ArMe^{\bullet+}$. This transfer produces $HS_8^{\bullet}$ and $ArCH_2^{\bullet}$ respectively. The formation of $ArCH_2^{\bullet}$ was proven indirectly – we have observed 1,2-diphenylethane as a major product when toluene oxidative thiolation was performed in neat (Table S1, entries 2,9). In this case, the concentration of $ArCH_2^{\bullet}$ radicals turns high enough to favour their recombination. In acetonitrile, in the next step C–S bond is created by recombination between the $HS_8^{\bullet}$ and $ArCH_2^{\bullet}$ radicals. A transition of hydropolysulfides to disulfides requires evolution of H_2S and extrusion of extra sulfur atoms, which in turn participates in subsequent reaction with ArMe. Apparently, K-PHI is also involved in all these steps, i.e. the polysulfides obviously react similarly to the original sulfur reactant. H_2S was detected as Ag_2S, when reaction mixture headspace was allowed to react with $AgNO_3$ (Fig. S4). Also traces of intermediate RCH_2SH were detected by GC-MS of the reaction mixture additionally supporting the mechanism (mass spectra, Fig. S5). Finally, the structure of K-PHI remains unaffected as proved by the identity of its PXRD patterns and FT-IR spectra before and after photocatalytic experiment (Fig. S6).

Conclusions

Potassium poly(heptazine imide) enables the photoredox thiolation of methylarenes with elemental sulfur. This reaction takes place under very mild conditions and blue light irradiation. The reaction proceeds *via* formation of polysulfides as intermediates, which potentially also could be isolated, if reaction is terminated at the appropriate time. The discovered photocatalytic conversion of methylarenes into disulfides clearly reflects the high oxidation power of K-PHI that activates the methyl C-H bond toward subsequent reaction with sulfur species. The mechanistic studies suggest that the reaction proceeds first *via* methylarene oxidation by photogenerated hole of K-PHI*, leaving a $K\text{-PHI}^{\bullet-}$ radical anion. We have isolated this long living $K\text{-PHI}^{\bullet-}$ radical anion and characterized spectroscopically. The exceptionally long life-time of the $K\text{-PHI}^{\bullet-}$ radical anion arises from its high stability under air-free conditions, as plausibilized by model calculations revealing a narrow band of delocalized states for the extra electron. All this make K-PHI a promising photo responsive material in energy storage applications. The newly disclosed reaction is convenient for the generation of a number of technically very useful disulfanes, as they, for instance, are used for rubber processing, surface modifications, or click chemical modifications of (bio)polymers. We expect the reaction to be more general and applicable to the oxidative modification of all C-H positions where the cation radical is resonance stabilized.

Experimental Section

^1H and ^{13}C NMR spectra were recorded on Agilent 400 MHz spectrometer using signal of TMS (0 ppm) as a reference. ^{13}C APT experiments were conducted to distinguish between C, CH_2 and CH, CH_3 carbon atoms. Agilent 6890 Network GC System coupled with Agilent 5975 Inert Mass Selective detector (electron ionization) were used for reaction mixture composition analysis and to obtain mass spectra of the products. Irradiance of the LED module was measured using PM400 Optical Power and Energy Meter equipped with integrating sphere S142C.

Synthetic procedures

***tert*-butyl *p*-tolylcarbamate** was prepared according to the literature procedure.[43] Mesoporous graphitic carbon nitride (mpg-CN) was prepared according to the literature procedure.[44]

K-PHI was prepared according to the literature procedure.[18] A mixture of 5-aminotetrazole (0.99 g) and LiCl/KCl eutectics (4.97 g) was brought together into a steel ball mill cup. The steel ball was placed and the cup was closed. The mixture of precursors has been grinded for 5 min at the shaking rate 25 s^{-1}. Resultant flour-like white powder was transferred into a porcelain crucible, covered with a porcelain lid and placed into the oven. The temperature inside the oven was increased from 20°C to 600°C within 4 hours under flow of nitrogen (15 L·min^{-1}) after which it was maintained at 600°C for another 4 hours. The oven was allowed to cool to room temperature. The melt from the crucible was transferred into a beaker; deionized water (50 mL) and stir bar were placed into a beaker. The suspension was kept at stirring at room temperature for 4 hours until suspension became fully homogeneous and no agglomerated particles were seen. Solid was separated by centrifugation (6500 min^{-1}, 12 min), washed with water (3x2 mL) using centrifuge to separate particles of the material (13500 min^{-1}, 1 min) and dried in vacuum giving 256 mg of the dark-yellow material.

A general procedure of methylarene oxidative thiolation: A screw-capped tube was charged with K-PHI (10 mg), methylarene (0.3 mL), elemental sulfur (0.96 mg, 30 μmol of S atoms) and acetonitrile (2.7 mL). The teflon coated stir bar was placed as well. The suspension was frozen in liquid nitrogen to solid state and evacuated till the residual pressure 0.1 mbar. The solid was warmed using the heating gun until the solid has melted. The procedure was repeated 3 times and the tube was finally refilled with argon. The suspension was vigorously stirred at +50°C under blue LED (461 nm, $0.0517\pm3\cdot10^{-5}$ W·cm^{-2}) irradiation for 24 hours. The reaction mixture was allowed to cool to room temperature and the tube was opened in the fume hood. Attention! Evolution of H_2S! Catalyst was separated by centrifugation (13000 min^{-1}) and washed with acetonitrile (3x1.5 mL). The washings were combined and acetonitrile evaporated under reduced pressure (+50°C, 80 mbar). The residue was washed with chloroform (3x2 mL) and undissolved particles were separated by centrifugation (13000 min^{-1}). Evaporation of chloroform under reduced pressure furnished corresponding disulfane.

1,2-dibenzyldisulfane. Yield: 56 %. ^1H, ^{13}C NMR, FT-IR spectra were identical to the authentic sample purchased from Acros Organics (Fig. S2). ^1H NMR (400 MHz, $CDCl_3$): δ = 3.60 (s, 4H,

View Article Online
DOI: 10.1039/C8SC00745D

CH_2), 7.23-7.34 (m, 10H, CH). ^{13}C NMR (400 MHz, $CDCl_3$): δ = 43.2 (s, CH_2), 127.4 (s, CH), 128.5 (s, CH), 129.4 (s, CH), 137.3 (s, CH). MS (EI): 246.1 (M^+).

1,2-bis(4-methoxybenzyl)disulfane. Yield: 67 %. ^{1}H NMR (400 MHz, $CDCl_3$): δ = 3.59 (s, 4H, CH_2), 3.80 (s, 6H, OCH_3), 6.85 (d, J_{HH}=8.8Hz, CH, 4H), 7.17 (J_{HH}=8.8Hz, CH, 4H). ^{13}C NMR (400 MHz, $CDCl_3$): δ = 42.7 (s, CH_2), 55.3 (s, OCH_3), 113.9 (s, CH), 129.4 (s, C), 130.5 (s, CH). MS (EI): 306.1 (M^+).

1,2-bis(2-methoxybenzyl)disulfane. Yield: 63 %. ^{1}H NMR (400 MHz, $CDCl_3$): δ = 3.76 (s, 4H, CH_2), 3.86 (s, 6H, OCH_3), 6.85-6.92 (m, 4H, CH), 7.16 (dd, J_{HH}=7.2Hz, J_{HH}=1.6Hz), 7.25 (dt, J_{HH}=1.6Hz, J_{HH}=8.0Hz). ^{13}C NMR (400 MHz, $CDCl_3$): δ = 38.3 (s, CH_2), 55.5 (s, OCH_3), 110.6 (s, CH), 120.2 (s, CH), 125.8 (s, C), 128.8 (s, CH), 131.0 (s, CH). MS (EI): 306.1 (M^+).

1,2-bis(1-phenylethyl)disulfane. Yield: 47 %. A mixture of diastereomers. ^{1}H NMR (400 MHz, $CDCl_3$): δ = 3.52 (q, J_{HH}=7.0Hz, 1H, CH), 3.60 (q, J_{HH}=7.0Hz, 1H, CH), 1.54 (d, J_{HH}=7.0Hz, 3H, CH), 1.55 (d, J_{HH}=7.0Hz, 3H, CH), 7.21-7.34 (m, 10H, CH). ^{13}C NMR (400 MHz, $CDCl_3$): δ = 20.4 (s, CH_3), 20.5 (s, CH_3), 49.4 (s, CH), 49.5 (s, CH), 127.4 (s, CH), 127.5 (s, CH), 127.7 (s, CH), 127.8 (s, CH), 128.3 (s, CH), 128.4 (s, CH), 142.4 (s, C), 142.4 (s, C). MS (EI): 274.1 (M^+).

1,2-bis(4-fluorobenzyl)disulfane. Yield: 41 %. ^{1}H NMR (400 MHz, $CDCl_3$): δ = 3.58 (s, 4H, CH_2), 7.01 (dd, J_{HH}=8.6Hz, J_{HH}=8.6 Hz, 4H, CH), 7.20 (dd, J_{HH}=5.4 Hz, J_{HH}=8.6 Hz, 4H, CH). ^{13}C NMR (400 MHz, $CDCl_3$): δ = 42.4 (s, CH_2), 115.4 (d, J_{CF}=21.5 Hz, CH), 130.9 (d, J_{CF}=8.1 Hz, CH), 162.2 (d, J_{CF}=246.4 Hz, CF). MS (EI): 282.0 (M^+).

di-tert-butyl((disulfanediylbis(methylene))bis(4,1-phenylene)) dicarbamate. Yield: 51 %. ^{1}H NMR (400 MHz, $CDCl_3$): δ = 1.51 (s, 18H, CH_3), 3.58 (s, 4H, CH_2), 6.46 (br. s., 2H, NH), 7.15 (d, J_{HH}=8.0 Hz, CH, 4H), 7.31 (d, J_{HH}=8.0 Hz, 4H, CH). ^{13}C NMR (400 MHz, $CDCl_3$): δ = 28.3 (s, CH_3), 42.8 (s, CH_2), 118.4 (s, CH), 130.0 (s, CH), 131.8 (s, C), 137.6 (s, C), 152.6 (s, C).

DFT calculations

The calculations were carried out in the GAMESS (US) program package[45], their results were visualized with the MacMolPlt graphical interface[46]. The poly(heptazine imide) matrix was modelled by a cluster comprised of 6 heptazine units linked by 4 =NH groups and 2 N atoms. Two K^+ cations were added to neutralize the negative charge of the matrix, which is originated from the deprotonated imide nitrogen atoms. To reduce computational cost, the symmetry of the model cluster was set to the C_{2v} point group. The basis was Dunning–Hay double zeta set with one *p*-type polarization function on hydrogen atoms and one *d*-type function on other atoms[46]. For the nitrogen atoms the basis set was additionally extended by a diffuse *sp*-shell. The geometry of K-PHI was optimized using 2 pure GGA functionals (PBE and BLYP) and 3 hybrids with different amount of Hartree–Fock exchange (25 % for PBE0, 20 % for B3LYP and 50 % for BHHLYP). The spatial distribution of the frontier orbitals in the cluster was found to be independent of the functional. On the other hand, the increase of the Hartree–Fock exchange percentage in the GGA < B3LYP < PBE0 < BHHLYP series increases the HOMO–LUMO gap by lowering the HOMO and raising the LUMO energies (see Table 1).

Conflicts of interest

There are no conflicts to declare.

Acknowledgements

The authors are grateful the Deutsche Forschungsgemeinschaft for the financial support (DFG-An 156 13-1) and thank Christian Wolff for measuring time-resolved PL spectra. A.M. acknowledges the financial support from the scholarship of the President of Ukraine for young scientists. Computing resources for DFT calculations were provided by the SCIT supercomputer (V.M. Glushkov Institute of Cybernetics of the NAS of Ukraine).[47]

Notes and references

‡ Due to the M+ effect of the methoxy group, oxidation potential of *p*-methylanisole is expected to be lower than that of toluene, 2.26 ± 0.02 V vs SCE.[29] Commonly used holes scavengers, alcohols, cannot be applied in this case as they were reported to react with MV^{2+}.[48]

1. J. A. Labinger and J. E. Bercaw, *Nature*, 2002, **417**, 507-514.
2. G. Zhang, Z.-A. Lan and X. Wang, *Angew. Chem. Int. Ed.*, 2016, **55**, 15712-15727.
3. J. Zhang, M. Zhang, R.-Q. Sun and X. Wang, *Angew. Chem. Int. Ed.*, 2012, **51**, 10145-10149.
4. Z. Lin and X. Wang, *Angew. Chem. Int. Ed.*, 2013, **52**, 1735-1738.
5. L. Lin, C. Wang, W. Ren, H. Ou, Y. Zhang and X. Wang, *Chem. Sci.*, 2017, **8**, 5506-5511.
6. Y. Zheng, L. Lin, X. Ye, F. Guo and X. Wang, *Angew. Chem. Int. Ed.*, 2014, **53**, 11926-11930.
7. R. Kuriki, O. Ishitani and K. Maeda, *ACS Appl. Mater. Interfaces*, 2016, **8**, 6011-6018.
8. F. Guo, P. Yang, Z. Pan, X.-N. Cao, Z. Xie and X. Wang, *Angew. Chem. Int. Ed.*, 2017, **56**, 8231-8235.
9. A. E. Shilov and G. B. Shul'pin, in *Activation and Catalytic Reactions of Saturated Hydrocarbons in the Presence of Metal Complexes*, KLUWER ACADEMIC PUBLISHERS, 2000, ch. 1.
10. Y. Wang, H. Li, J. Yao, X. Wang and M. Antonietti, *Chem. Sci.*, 2011, **2**, 446-450.
11. S. Verma, R. B. N. Baig, M. N. Nadagouda and R. S. Varma, *ACS Sustainable Chem. Eng.*, 2016, **4**, 2333-2336.
12. A. Henríquez, H. D. Mansilla, A. M. M.-d. l. Cruz, J. Freer and D. Contreras, *Appl. Catal., B*, 2017, **206**, 252-262.
13. M. A. Gonzalez, S. G. Howell and S. K. Sikdar, *J. Catal.*, 1999, **183**, 159-162.
14. D. Dontsova, S. Pronkin, M. Wehle, Z. Chen, C. Fettkenhauer, G. Clavel and M. Antonietti, *Chem. Mater.*, 2015, **27**, 5170-5179.
15. A. Savateev, S. Pronkin, J. D. Epping, M. Willinger, C. Wolff, D. Neher, M. Antonietti and D. Dontsova, *ChemCatChem*, 2017, **9**, 167–174.
16. X. Wang, K. Maeda, A. Thomas, K. Takanabe, G. Xin, J. M. Carlsson, K. Domen and M. Antonietti, *Nat. Mater.*, 2009, **8**, 76 - 80

View Article Online
DOI: 10.1039/C8SC00745D

17. A. Savateev, S. Pronkin, J. D. Epping, M. G. Willinger, M. Antonietti and D. Dontsova, *J. Mater. Chem. A*, 2017, **5**, 8394-8401.
18. A. Savateev, D. Dontsova, B. Kurpil and M. Antonietti, *J. Catal.*, 2017, **350**, 203–211.
19. B. Kurpil, K. Otte, M. Antonietti and A. Savateev, *Appl. Catal., B*, 2018, **228**, 97-102.
20. B. Kurpil, B. Kumru, M. Antonietti and A. Savateev, *Green Chemistry*, 2018, **20**, 838-842.
21. B. Kurpil, A. Savateev, V. Papaefthimiou, S. Zafeiratos, T. Heil, S. Özenler, D. Dontsova and M. Antonietti, *Appl. Catal., B*, 2017, **217**, 622-628.
22. R. Godin, Y. Wang, M. A. Zwijnenburg, J. Tang and J. R. Durrant, *J. Am. Chem. Soc.*, 2017, **139**, 5216-5224.
23. V. W.-h. Lau, D. Klose, H. Kasap, F. Podjaski, M.-C. Pignié, E. Reisner, G. Jeschke and B. V. Lotsch, *Angew. Chem.*, 2016, **56**, 510-514.
24. F. Podjaski, J. Kröger and B. V. Lotsch, *Adv. Mater.*, 2018, **30**, 1705477.
25. Z. Chen, A. Savateev, S. Pronkin, V. Papaefthimiou, C. Wolff, M. G. Willinger, E. Willinger, D. Neher, M. Antonietti and D. Dontsova, *Adv. Mater.*, 2017, **29**, 1700555.
26. A. Savateev, S. Pronkin, M. Willinger, M. Antonietti and D. Dontsova, *Chem. - Asian J.*, 2017, **12**, 1517-1522.
27. G. Zhang, G. Li, Z.-a. Lan, L. Lin, A. Savateev, T. Heil, S. Zafeiratos, X. Wang and M. Antonietti, *Angew. Chem. Int. Ed.*, 2017, **56**, 13445-13449.
28. T. Watanabe and K. Honda, *J. Phys. Chem.*, 1982, **86**, 2617-2619.
29. P. B. Merkel, P. Luo, J. P. Dinnocenzo and S. Farid, *J. Org. Chem.*, 2009, **74**, 5163-5173.
30. A. M. Roy, G. C. De, N. Sasmal and S. S. Bhattacharyya, *Int. J. Hydrogen Energy*, 1995, **20**, 627-630.
31. M. Bouroushian, in *Monographs in Electrochemistry*, Springer-Verlag, Berlin Heidelberg, 2010, vol. 1, ch. 1, pp. 57-75.
32. G. Kutney, *Sulfur. History, Technology, Applications and Industry*, ChemTec Publishing, 2007.
33. W. J. Chung, J. J. Griebel, E. T. Kim, H. Yoon, A. G. Simmonds, H. J. Ji, P. T. Dirlam, R. S. Glass, J. J. Wie, N. A. Nguyen, B. W. Guralnick, J. Park, Á. Somogyi, P. Theato, M. E. Mackay, Y.-E. Sung, K. Char and J. Pyun, *Nat. Chem.*, 2013, **5**, 518-524.
34. J. Lim, J. Pyun and K. Char, *Angew. Chem.*, 2015, **54**, 3249-3258.
35. R. Ballini, *Synthesis*, 1982, **1982**, 834-836.
36. K. L. Stensaas, A. S. Brownell, S. Ahuja, J. K. Harriss and S. R. Herman, *J. Sulfur Chem.*, 2008, **29**, 433-443.
37. A. U. Meyer, V. W.-h. Lau, B. König and B. V. Lotsch, *Eur. J. Org. Chem.*, 2017, **2017**, 2179–2185.
38. A. J. Kamyshny, A. Goifman, J. Gun, D. Rizkov and O. Lev, *Environ. Sci. Technol.*, 2004, **38**, 6633-6644.
39. B. Eckert and R. Steudel, in *Elemental Sulfur und Sulfur-Rich Compounds II*, ed. R. Steudel, Springer Berlin Heidelberg, Berlin, Heidelberg, 2003, DOI: 10.1007/b13181, pp. 31-98.
40. A. M. d. P. Nicholas and D. R. Arnold, *Can. J. Chem.*, 1982, **60**, 2165-2179.
41. R. Breslow and J. L. Grant, *J. Am. Chem. Soc.*, 1977, **99**, 7745-7746.
42. T. Chivers and I. Drummond, *Inorg. Chem.*, 1972, **11**, 2525-2527.
43. T. Ishida, S. Kikuchi, T. Tsubo and T. Yamada, *Org. Lett.*, 2013, **15**, 848-851.
44. F. Goettmann, A. Fischer, M. Antonietti and A. Thomas, *Angew. Chem. Int. Ed.*, 2006, **45**, 4467-4471.
45. M. W. Schmidt, K. K. Baldridge, J. A. Boatz, S. T. Elbert, M. S. Gordon, J. H. Jensen, S. Koseki, N. Matsunaga, K. A. Nguyen, S. Su, T. L. Windus, M. Dupuis and J. A. M. Jr, *J. Comput. Chem.*, 1993, **14**, 1347-1363.
46. B. M. Bode and M. S. Gordon, *J. Mol. Graphics Modell.*, 1998, **16**, 133-138.
47. A. L. Holovynsky, A. L. Malenko and I. V. Sergienko, *Visn. Nac. Acad. Nauk Ukr.*, 2013, 50-59.
48. J. G. Carey, J. F. Cairns and J. E. Coxhewer, *Journal of Chemical Society D*, 1969, **0**, 1280-1281.

View Article Online
DOI: 10.1039/C8SC00745D

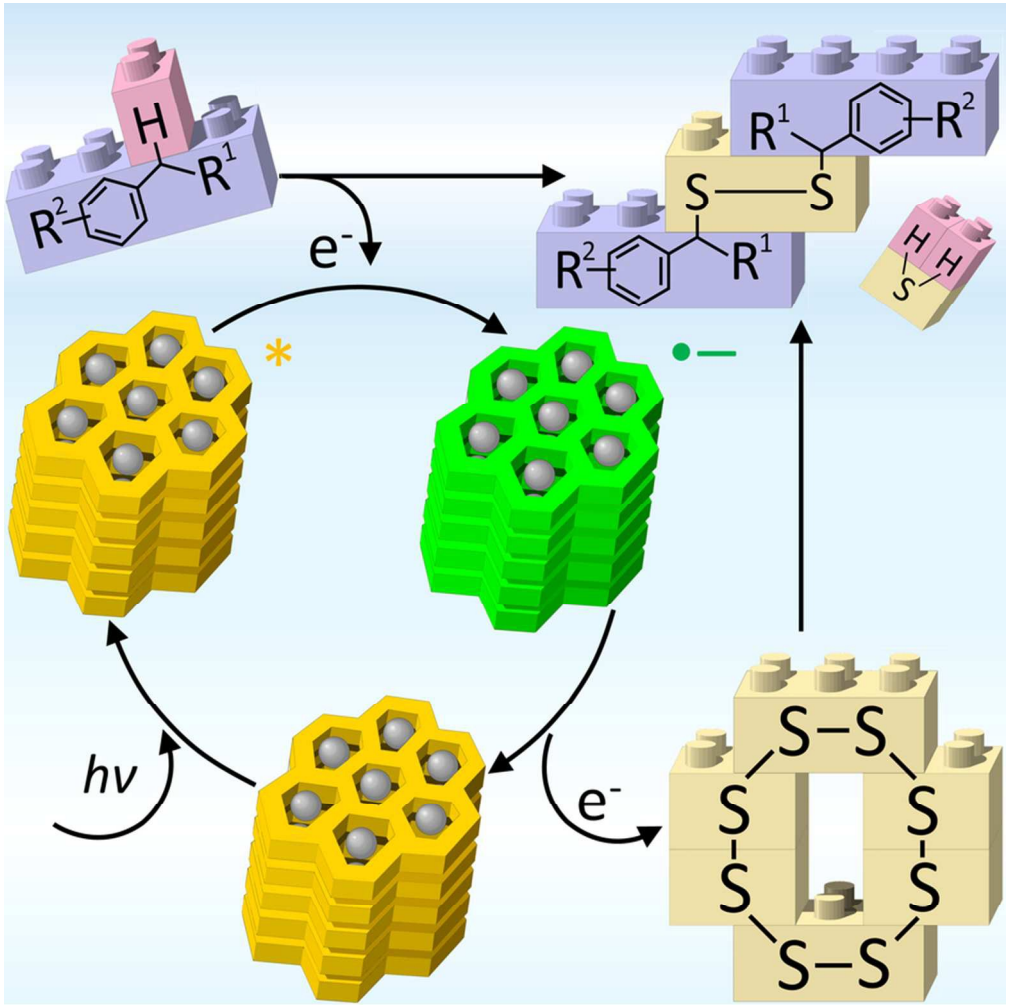

39x39mm (600 x 600 DPI)